

The Properties of Satellite Galaxies in External Systems. II. Photometry and Colors

Carlos M. Gutiérrez

Instituto de Astrofísica de Canarias, E-38205 La Laguna, Tenerife, Spain

cgc@ll.iac.es

and

Marco Azzaro

Isaac Newton Group of Telescopes, Ap. 321, E-38700 S/C de La Palma, La Palma, Spain

ABSTRACT

In this second paper dedicated to the study of satellite galaxies we present broad-band photometry in the B , V , R and I filters of 49 satellite galaxies orbiting giant isolated spiral galaxies. First analysis of the properties of these objects are presented by means of color-color and color-magnitude diagrams for early- and late-type satellites. Although we find differences in the slope of the $V - I$ vs. M_v color magnitude diagram, as a whole, the relations are in agreement with the trends known to date for galaxies of similar magnitudes in nearby clusters of galaxies. Comparison with the relations found for satellites in the Local Group allows us to sample better the bright end of the luminosity function of satellite galaxies and extends for brighter objects the validity of the color-magnitude relation found for dwarf galaxies in the Local Group. Most of the E/S0 galaxies in our sample show a negative color gradient with values similar to those known for early type galaxies in other environments.

Subject headings: galaxies: fundamental parameters, galaxies: photometry, galaxies: structure, galaxies

1. Introduction

The study of the small scale structure in the Universe is a much discussed topic in current astronomy. One of the reasons for this wide interest is the discrepancies between observations

and the predictions of the standard cold dark matter (CDM) model. For instance, from n -body simulation (Moore et al. 1999; Klypin et al. 1999) the expected number of satellites orbiting galaxies like the Milky Way or Andromeda is an order of magnitude larger than that observed in the Local Group (e.g., Mateo 1998). This is a potentially strong objection against the hierarchical scenario proposed in the standard CDM model. To solve this discrepancy several mechanisms that suppress the formation of satellites after the re-ionization in the early epoch of the Universe have been proposed (e.g., Bullock, Kravtsov, & Weinberg 2000). So far, it is unclear whether this or any of the other mechanisms proposed is able to reconcile fully the predictions from the models and the observations.

Satellite galaxies are also interesting for tracing the gravitational potential and for estimating the mass of the parent galaxy at distances unreachable with other methods (Erickson, Gottesman & Hunter 1999). The standard models predict a decline in satellite galaxy velocity with distance to the primary. This has been observationally explored by Zaritsky et al. (1997) and Prada et al. (2003). The predicted effect was not found in the analysis of the first group. However, Prada et al., with better statistics and the removal of interlopers, have claimed the existence of this decline in the way predicted by the standard models.

Our knowledge of satellite galaxies beyond the Local Group is still very limited, owing to the intrinsic faintness of these objects. For instance, in the Local Group the known dwarf satellite galaxies have brightnesses in the range $-18 \leq M_B \leq -8$. So detailed studies of external systems are limited to galaxies in the nearby Universe. Even surveys such as the Sloan Digital Sky Survey (Prada et al. 2003) are capable to sampling only the very bright part of the luminosity function of these objects, typically detecting 1–2 satellites orbiting each giant galaxy. For instance, the external isolated galaxies in which a larger number of galaxies have been found are NGC 1961 (Gottesman, Hunter & Shostak 1993) and NGC 5084 (Carignan et al. 1997) in which 5 and 9 satellites respectively have been catalogued.

Bearing all the above points in mind, we decided to start a study of satellite galaxies orbiting external isolated galaxies. We extracted our sample from the compilation of such objects by Zaritsky et al. (1997). Only spiral parents were included in that catalogue. A similar catalogue for parents with elliptical morphologies is being compiled by Smith & Martinez (2003). With photometry in optical broad ($BVRI$) and narrow bands ($H\alpha$), and near infrared (J and K) of both the satellites and their parent galaxies we address the following questions: i) what are the properties (statistics, luminosity function, morphology, structure, colors, etc.) of the satellite galaxies, and how do they compare with those found in the Local Group; ii) how the above properties are related to the relative positions of the satellite galaxies with respect to their parents; iii) what the possible interactions are between satellites, and between satellites and their parents; and iv) the star formation rate and how

it is related with the overall properties and relative position of the satellites. In the first paper of this series, Gutierrez, Azzaro, & Prada (2002, hereafter Paper I), we presented the structural parameters and morphological classification of ~ 60 of such objects. Here, we present the photometry and first analysis of the colors of most of them. A full analysis combining structure and photometry and testing against the predictions of theoretical models will be conducted and presented in the near future.

2. Observations and Photometry

The observations presented here were performed during several runs at the IAC80,¹ the Nordic Optical Telescope (NOT),² and the 1.23 and 2.2 m Calar Alto³ telescopes. The details of the sample can be found in Zaritsky et al. (1997) and Paper I. Typical integration times per filter and galaxy range from ~ 30 to ~ 90 minutes on the IAC80, and from ~ 5 to ~ 30 min on the other telescopes. The seeing was between 1.5 and 2.0 arcsec in most cases. The observations were usually performed in photometric conditions and calibrated using Landolt stars (Landolt 1992). In a few cases of non-photometric nights we made relative calibrations with photometric nights using bright field stars (typically 4–8 in each case). The typical rms accuracy of the calibration is ~ 0.03 mag. The data were reduced using IRAF.⁴ More details on the observations and reduction can be found in Paper I. The magnitudes presented here were computed using the software SExtractor (Bertin & Arnouts 1996) and correspond to the total integrated magnitudes computed in apertures defined in the way proposed by Kron (1980). The uncertainty in the estimation of these magnitudes are dominated by the sky subtraction and the extrapolation of the external profile of the galaxies. We estimate the typical overall uncertainty as ~ 0.1 mag.

Table 1 presents the integrated photometry in the four bands. We have photometry for 49 objects, $\sim 80\%$ of them in all four bands. For most of them we have also analyzed the

¹The IAC-80 is located at the Spanish Teide Observatory on the island of Tenerife and is operated by the Instituto de Astrofísica de Canarias.

²The Nordic Optical Telescope is operated on the island of La Palma jointly by Denmark, Finland, Iceland, Norway, and Sweden, in the Spanish Roque de los Muchachos of the Instituto de Astrofísica de Canarias Observatory.

³The German-Spanish Astronomical Centre, Calar Alto, is operated by the Max-Planck-Institute for Astronomy, Heidelberg, jointly with the Spanish National Commission for Astronomy.

⁴IRAF is the Image Reduction and Analysis Facility, written and supported by the IRAF programming group at the National Optical Astronomy Observatory (NOAO) in Tucson, Arizona.

morphology and structure (see Paper I). The galaxies span a range of ~ 6 mag in apparent magnitude. When converted to absolute magnitudes, this range is ~ 5 mag, i.e., a factor of ~ 100 in mass.

We have made a comparison between the M_B magnitudes presented by Zaritsky et al. and our estimate in this band. To obtain the absolute magnitudes from our measurements we have used a value of the Hubble constant of $72 \text{ km s}^{-1} \text{ Mpc}^{-1}$. We have excluded in this comparison the object NGC 5965a because we have found two objects (denoted as NGC 5965a1 and NGC 5965a2 in Table 1) that are very close together (the angular distance between them is 1.6 arcsec), and it is unclear if the magnitude quoted by Zaritsky et al. corresponds to one of the two components or to the combination of both. The objects show evidence of interaction, so we think that both are satellites of NGC 5965. After these objects were excluded, we have 39 objects with measurements in the B band. The absolute magnitude in the B band Zaritsky et al. (denoted here by M_{Bz}) were slightly modified in order to take into account the different values of the Hubble constant used by these authors and by us (75 and $72 \text{ km s}^{-1} \text{ Mpc}^{-1}$ respectively). In Figure 1 we present this comparison. The differences are $\Delta = |M_B - M_{Bz}| \leq 1$. The figure shows no systematic error, the mean value of the residuals being 0.31 mag and the rms 0.45 mag. Considering that the magnitudes reported by Zaritsky et al. are photographic, and that these authors estimated a proper uncertainty of ± 0.5 mag, we conclude that both estimates are in very good agreement. This comparison also indicates that our uncertainties in the estimation of the magnitudes are small compared with the above value.

3. The Color–Magnitude Relation for Satellite Galaxies

The existence of a color–magnitude relation for elliptical galaxies in clusters is widely known (e.g., Visvanathan & Sandage 1977). The origin of this relation is controversial: while some authors (Kodama & Arimoto 1997) have argued that the relation is a consequence of changes in metallicity, others (Ferreiras, Charlot, & Silk 1999) think that it is a consequence of changes in both age and metallicity. Recently (Vazdekis et al. 2001) have analyzed high signal-to-noise ratio spectra of six elliptical galaxies in the Virgo Cluster using a new spectral index, and conclude that the color–magnitude relation is a consequence of a relation between luminosity (or mass) and metallicity. For the analysis presented in this section, we have corrected the magnitudes quoted in Table 1 for Galactic extinction using the model by Schlegel, Finkbeiner, & Davis (1998).

Figure 2 presents a color–magnitude diagram for the galaxies classified as early and late types in our sample. The objects span a range of ~ 4 mag while they are in a narrow range

in the $B - V$ and $V - I$ colors. Although the statistics are poor because of the low number of objects analyzed, the existence of a tight relation between colors and magnitudes is clear. This color–magnitude relation is similar for both types of galaxies (early and late), although it is notable that the dispersion of the early types with respect to these relations is smaller. The mean values are +0.70 and +0.65 for the $B - V$ colors, and +0.93 and +0.88 for the $V - I$ colors of early and late types respectively. For these two type of galaxies we have conducted least squares fits of the equations $B - V = aM_V + b$ and $V - I = aM_V + b$ respectively. For these fits we assigned the same weight to all galaxies. The parameters of these fits are presented in Table 2. Combining the two colors $B - V$ and $V - I$, we obtain the color–color diagram presented in Figure 3. As expected from the previous figure, galaxies tend to occupy a narrow region in this diagram, with the brightest galaxies being redder than the faintest ones. Roughly speaking, the position (0.8, 1.0) in the ($B - V$, $V - I$) plane separates galaxies with $M_B \leq -18$ from those with $M_B \geq -18$. We have compared these results with those found for galaxies with similar magnitudes in the Fornax Cluster by Karick, Drinkwater, & Gregg (2003), and Griensmith (1982). We note similar trends but with a larger dispersion in our objects; and a reddening with luminosity similar in the $B - V$ colors and larger in $V - I$ for the galaxies of our sample. For instance, Karick et al. obtained mean values of $B - V$ of 0.70 and 0.57 for their sample of dwarf ellipticals and late types. These values are roughly compatible with those that we have obtained. The small discrepancy found between the $B - V$ colors of late types is partially due to the different magnitude range of galaxies in both samples. Karick et al. obtained a slope for the $B - V$ relation of the early type population of -0.034 ± 0.006 ; this and the value found by Griensmith (1982) are compatible with our results. However the slope obtained for the $V - I$ curve is different between the Fornax members and the objects analyzed here. The slope of this color-magnitude relation is larger in our sample. If we restrict our analysis to the common range in magnitude between both samples, this difference persists. Possible reasons for this difference will be analyzed in a future paper.

We have compared the photometric properties of the satellites of our sample with those found for galaxies in the Local Group. The values for the photometric integrated magnitudes have been taken from the compilation by Mateo (1998) and correspond to all the members of the Local Group known by that time, apart of the Milky Way, M31, and the two Magellanic clouds which have been excluded from the analysis. This is illustrated in Figure 4 in which we present the color–magnitude diagram for both sets of objects. The typical uncertainties for our measurements in B and V are ~ 0.1 mag (when the colors are computed part of the systematic errors cancel out). In this figure we have also included a few objects for which we do not have a morphological classification and so excluded them from Figure 2. For the Local Group galaxies the uncertainties in the colors are ~ 0.05 while, according

to the compilation by Mateo (1998), the uncertainty is, in general, large for the integrated magnitudes. Although we have not represented these errors, they are not essential for making a qualitative analysis of the figure. We see how the external satellites correspond to the brightest part of the Local Group luminosity function, and also to some brighter satellites with luminosities similar to that of M33. This is expected because of the way in which the original sample by Zaritsky et al. was built. Galaxies within the common range of magnitudes have similar $B - V$ color and dispersions. The least-squares fit of $B - V$ vs. M_B obtained for the early-type external satellites seems also to fit notably well the galaxies of the Local Group. This extends the validity of this color–magnitude relation through a range of 12 magnitudes and demonstrates the universal nature of the color–magnitude relation for satellite galaxies.

4. Internal Color Gradients of Early-Type Satellites

The existence of color gradients in early-type galaxies is well known. In general, elliptical galaxies tend to be redder in their inner regions. As for the color–magnitude relation, the effect could be explained by either a gradient in stellar age or metallicity, or by a combination of both. The existence of dust more concentrated in the central parts of the galaxy could also contribute totally or partially to the observed color gradients. The first studies for giant ellipticals using CCD measurement were conducted by Franx & Illingworth (1990), Peletier et al. (1990), and de Jong (1996). Using the *Hubble Space Telescope*, this study has been extended to galaxies at higher redshift (Moth & Elston 2002), who show the existence of negative gradients at intermediate ($0.5 \leq z \leq 1.2$) redshifts, while the gradients become very positive at higher ($2.0 \leq z \leq 3.5$) redshifts.

We have analyzed the gradients of the 16 galaxies classified as E or E/S0 in the morphological analysis presented in Paper I. Considering the angular size of the objects and the limiting magnitude and spatial resolution of our data, we decided to conduct a very simple analysis in the following way: i) we checked the value of the seeing in both filters (in cases of significant different values, the image in the filter with best seeing was convolved with a Gaussian of appropriate width to match in the convolved image the seeing in the other filter), ii) we selected the angular range between $2 \times$ FWHM and the radius which encloses the full galaxy and computed the integrated magnitudes in several concentric apertures within this range, and iii) we did a linear least-squares fit of $B - R$ vs. $\log r$. The slope of this relation is denoted by $\Delta(B - R)/\Delta(\log r)$ and is presented in Table 3. In some cases we check the behavior of this gradient with that obtained using other colors (usually $V - I$).

A few galaxies were excluded from this analysis for the reasons detailed below: NGC 895a,

which has an off-center nucleus and is also a rather compact object with an angular size too small to compute the gradients; NGC 2718*a*, which, apart from being an object in clear interaction with NGC 2718*b*, has another object very close to it (we were able to separate it from the main galaxy in the photometric analysis presented in this paper, but not in this estimate of gradients); NGC 5962*a*, whose angular size is too small with respect to the seeing; A910*a* and NGC 2939*a* because we have observed them in only one filter; and NGC 4541*b*, which is in clear interaction with NGC 4541*e* and whose gradients shows a complex dependence on radius. We have also included the galaxy NGC 3735*b*, classified as early type in Paper I, but which is not included in Table 1 because of the lack of calibrated observations of this galaxy. After this selection, we were left with nine objects, whose results are presented in Table 3. Seven of the nine galaxies have negative slopes, while NGC 488*a* has a value very close to 0 and, surprisingly, NGC 4725*b* shows an extremely positive gradients (i.e., the outer parts are notably redder than the inner ones. We have checked this trend measuring the gradients in other colors and obtained the same tendency. Positive gradients such as this are uncommon in low redshift galaxies and probably indicate strong star formation in the central part of the galaxy. This galaxy is rather regular, and so far, we have not found any clear evidence of distortions associated with any interactions or mergers that could trigger this burst. The mean value of the gradient (excluding NGC 4725*b*) is $\Delta(B - R)/\Delta(\log r) = -0.085 \pm 0.027$.

5. Summary

1. We have presented integrated photometry of 49 satellite galaxies orbiting external isolated spiral galaxies.
2. The $B - V$ vs. M_V color magnitude relation is similar to the one found in the Fornax Cluster for galaxies with similar magnitudes. However the $V - I$ vs. M_V relation is steeper in our sample as compared with galaxies in Fornax.
3. The $B - V$ vs. M_B color diagram extends to brighter magnitudes the relations found for satellite galaxies in the Local Group.
4. We have measured the internal color gradients of nine early-type satellites. Excluding a galaxy with a strong positive gradient, we found $\Delta(B - R)/\Delta(\log r) = -0.085 \pm 0.027$.

We would like to thank Francisco Prada for fruitful and encouraging discussions. We also thank the anonymous referee for useful comments.

REFERENCES

- Bertin, E., & Arnouts, S. 1996, *A&A*, 117, 393
- Bullock, J. S., Kravtsov, A. V., & Weinberg, D. H. 2000, *ApJ*, 539, 517
- Carignan, C., Cote, S., Freeman, K. C., & Quinn, P. J. 1997, *AJ*, 113, 1585
- de Jong, R. S. 1996, *A&A*, 313, 377
- Erickson, L. K., Gottesman, S. T., & Hunter, Jr., J. H. 1999, *ApJ*, 515, 153
- Ferreras, I., Charlot, S. & Silk, J. 1999, *ApJ*, 521, 81
- Franx, M., & Illingworth, G. 1990, *ApJ*, 359, L41
- Gottesman, S. T., Hunter, Jr., J. H., & Shostak, G. S. 1993, *MNRAS*, 212, p21
- Griersmith, D. 1982, *ApJ*, 87, 462
- Gutierrez, C. M., Azzaro, M., & Prada, F. 2002, *ApJS*, 141, 61 (Paper I)
- Karick, A. M., Drinkwater, M. J., & Gregg, M. D. 2003, *MNRAS*, 344, 188
- Klypin, A., Kravtsov, A. V., Valenzuela, O., & Prada, F. 1999, *ApJ*, 522, 82
- Kodama, T. & Arimoto, Y. 1997, *A&A*, 320, 41
- Kron, R. G. 1980, *ApJS*, 43, 305
- Landolt, A. U. 1992, *A&A*, 104, 340
- Mateo, M. L. 1998, *ARA&A*, 36, 435
- Moore, B., Ghigna, S., Governato, F., Lake, G., Quinn, T., Stadel, J., & Tozzi, P. 1999,,
ApJ, 524, L19
- Moth, P., & Elston, R. J. 2002, *ApJ*, 124, 1886
- Peletier, R. F., Davies, R. L., Illingworth, G. D., Davis, L. E., & Cawson, M. 1990, *AJ*, 100,
1091
- Prada, F. et al. 2003, *ApJ*, 598, 260
- Smith, R. M., & Martinez, V. 2003, proceedings of the "Satellite galaxies and tidal streams", eds. F. Prada, D. Martínez-Delgado and T. Mahoney. ASP Conf. Ser. astro-ph/0309818

Schlegel, D. J., Finkbeiner, D. P., & Davis, M. 1998, *ApJ*, 500, 525

Vazdekis, A., Kuntschner, H., Davies, R. L., Arimoto, N., Nakamura, O., & Peletier, R.
2001, *ApJ*, 551, L127

Visvanathan, N., & Sandage, A. 1977, *ApJ*, 216, 214

Zaritsky, D., Smith, R., Frenk, C., & White, S. D. M. 1997, *ApJ*, 478, 39

Table 1:: Integrated photometry of satellite galaxies. The columns are: 1) name of the object; 2) recessional velocity of the parent galaxy (from Zaritsky et al. 1997); 3-6) B , V , R , and I integrated magnitudes; telescope (1. IAC80, 2 NOT, 3. 1.23 m Calar Alto, 4. 2.2 m Calar Alto).

Object	V (km s $^{-1}$)	B	V	R	I	Telescope
NGC 259b	3808	15.04	14.37	13.83	13.30	1
NGC 488a	2268	15.39	14.48	13.93	13.34	1
NGC 488b	2268	16.18	15.63	15.29	14.99	1
NGC 488c	2268	16.60	15.61	15.22	14.62	1
I1723a	5531	19.45	18.85	17.99	18.10	1
I1723b	5531	16.94	16.08	15.53	14.91	1
NGC 749a	4406	—	—	15.59	—	1
NGC 749b	4406	—	—	16.93	—	1
NGC 772a	2468	14.42	13.49	12.86	12.19	1
NGC 772b	2468	—	—	15.55	15.08	1
NGC 772c	2468	16.22	15.43	14.88	14.42	1
NGC 895a	2290	—	16.72	16.49	16.13	1
NGC 1517a	3483	16.54	15.77	15.11	14.74	1
NGC 1620a	3513	—	15.17	14.27	—	1
NGC 1620b	3513	14.91	13.91	13.26	12.74	1
NGC 1961a	3934	14.98	14.14	13.52	12.73	4
NGC 1961b	3934	15.82	14.88	14.25	13.38	4
NGC 1961c	3934	14.94	14.18	13.66	12.80	4
NGC 1961d	3934	14.81	14.22	13.51	12.95	1
NGC 1961e	3934	15.64	—	12.71	12.17	1
NGC 2718a	3842	17.32	16.71	16.44	16.14	3
NGC 2718b	3842	16.23	15.69	15.26	14.88	3
NGC 2775a	1357	15.48	14.87	14.59	14.28	2
NGC 4162a	2561	16.81	16.10	15.58	15.12	2
NGC 4541a	6898	16.45	15.72	15.11	14.43	3
NGC 4541b	6898	16.71	16.16	15.36	14.84	3
NGC 4541d	6898	17.07	16.44	16.03	15.65	3
NGC 4541e	6898	15.62	14.95	14.37	13.87	3
A1242a	6301	17.11	16.56	16.37	16.20	2

NGC 4725a	1207	13.01	12.33	11.88	11.27	3
NGC 4725b	1207	15.80	15.14	14.71	14.26	2
NGC 5248a	1154	15.25	14.72	14.57	14.34	1
NGC 5324b	3044	16.60	16.06	15.68	15.37	2
A1416a	6809	16.09	14.96	14.35	13.72	2
NGC 5899a	2563	14.43	13.39	12.67	11.95	1
NGC 5921a	1478	15.66	—	14.38	—	1
NGC 5965a1	3413	16.29	15.86	15.54	15.20	2
NGC 5965a2	3413	17.19	16.50	16.60	16.29	2
NGC 5962a	1955	—	17.50	16.92	16.08	1
NGC 5962d	1955	15.55	14.78	14.33	13.72	1
NGC 6181a	2371	14.46	13.75	13.23	12.69	2
NGC 6384a	1655	14.24	12.94	12.61	12.00	1
NGC 7137a	1691	—	—	16.27	15.52	1
NGC 7177a	1150	14.56	13.85	13.22	12.55	1
NGC 7184a	2632	18.48	17.16	16.71	15.98	1
NGC 7290a	2900	17.00	16.51	16.05	16.17	1
NGC 7290b	2900	16.97	16.17	15.83	15.25	1
NGC 7678a	3486	15.30	14.86	14.35	13.94	1
NGC 7755a	2961	17.83	—	—	17.15	1

Table 2: Color-magnitude relations for satellite galaxies.

Color	Type	N	a	b	σ
$B - V$	Early	11	-0.048 ± 0.019	-0.158	0.140
	Late	22	-0.049 ± 0.012	-0.241	0.185
$V - I$	Early	12	-0.138 ± 0.017	-1.539	0.173
	Late	22	-0.193 ± 0.013	-2.650	0.249

Table 3: Color gradients for early-type satellite galaxies.

Galaxy	Range (arcsec)	$\Delta(B - R)/\Delta(\log r)$ (mag arcsec ⁻²)
NGC 259b	2 – 8	-0.031
NGC 488a	2 – 6	+0.009
I1723b	2 – 6	-0.056
NGC 772a	2 – 7	-0.076
NGC 1620b	2 – 7	-0.121
NGC 2718b	2 – 5	-0.216
NGC 3735b	2 – 7	-0.169
NGC 4725b	2 – 7	+0.621
NGC 7290b	2 – 4	-0.023

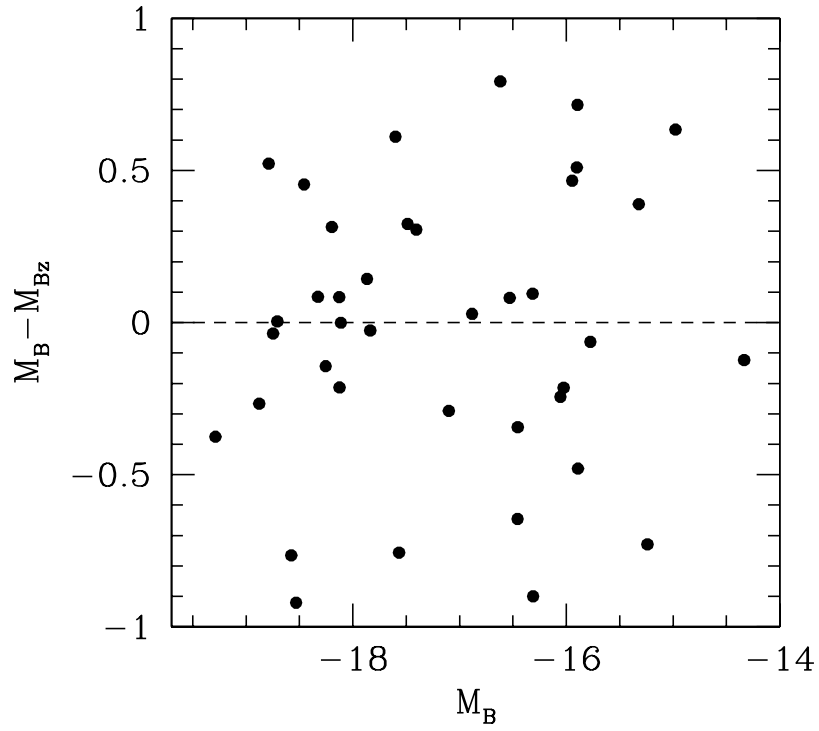


Fig. 1.— Comparison between the absolute magnitudes derived by Zaritsky et al. (1997) (M_{Bz}) and those (M_B) derived from the observations presented in this paper.

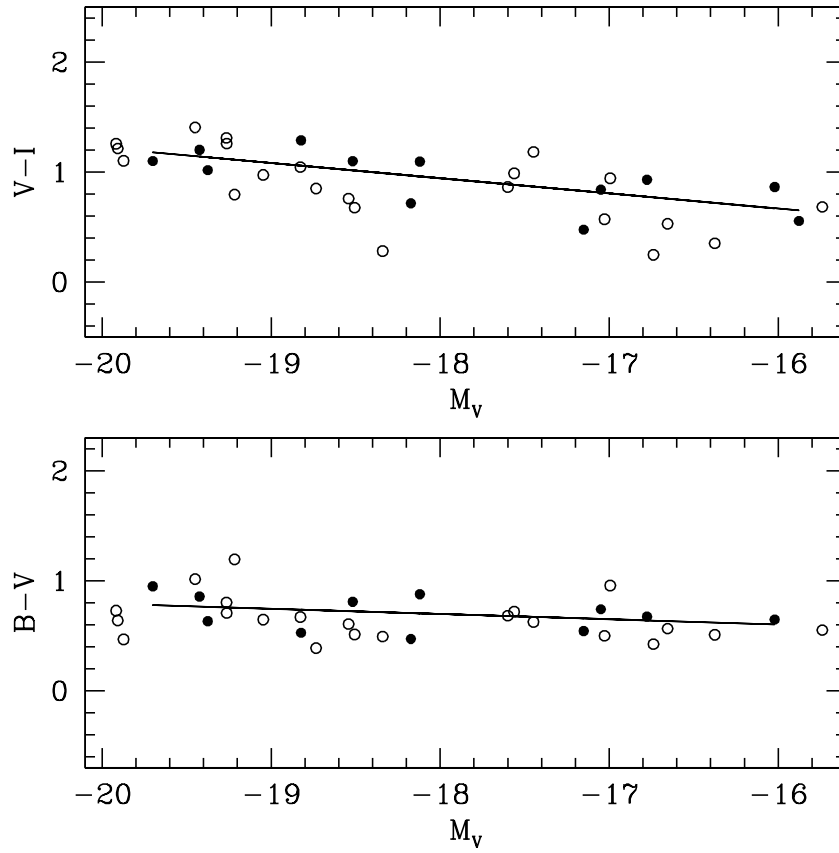


Fig. 2.— Color-magnitude diagrams for early type (*filled circles*) and late type (*open circles*) satellite galaxies. The lines are least-squares fits to the early type galaxies.

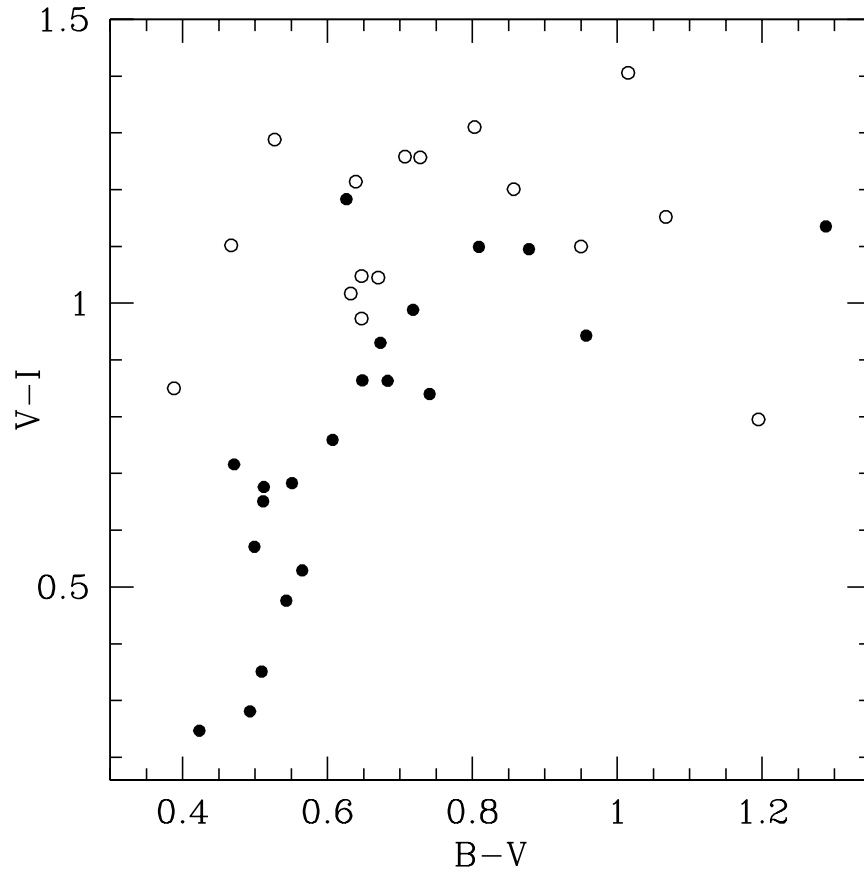


Fig. 3.— Color-color diagram of the satellite galaxies with $M_B \leq -18$ (*open circles*) and $M_B \geq -18$ (*filled circles*).

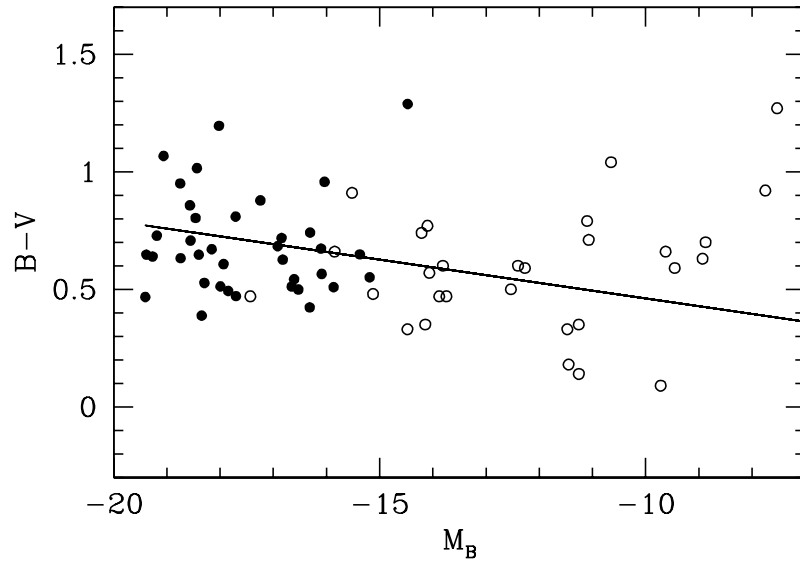


Fig. 4.— Color–magnitude diagram of the satellite galaxies presented in this article (*filled circles*) and the dwarf galaxies of the Local Group (*open circles*). The line is a least-squares fit to the external early type satellite galaxies.